Response letter of manuscript ESSD-2025-807

25-year, quarterly land change maps of China's Loess Plateau reveal long-term and substantial water-induced soil erosion mitigation

Authors: **Mofan Cheng, Zhuohong Li, Linxin Li, Wei He[†], Liangpei Zhang, and Hongyan Zhang[†]**

Dear Editors and Reviewers:

The authors would like to thank the editors and reviewers for their constructive comments and suggestions that have helped improve the quality of this manuscript. The manuscript has undergone a thorough revision according to the editors and reviewers' comments. Please see our responses below. For the reviewers' convenience, we have highlighted significant changes in the revised manuscript in blue.

Reviewer 1

This manuscript presents a substantial advancement in both methodology and data availability for investigating soil erosion dynamics in fragile ecosystems, with a particular focus on the Loess Plateau. By integrating long-term time-series Landsat and Sentinel imagery with relevant environmental datasets, the authors develop a high-resolution land-cover and soil erosion dataset spanning 25 years, while further shortening the update frequency to a quarterly scale. Such temporal coverage and resolution represent a notable improvement over existing regional product. The reported mapping performance is robust for a large-scale application, with an overall accuracy of 81.44% for land-cover classification and a mean absolute error of 4.5% for soil erosion estimates. Based on an examination of the released dataset, this work is expected to provide a valuable data foundation for future studies on land-surface processes, ecological restoration, and environmental change across the Loess Plateau. Leveraging this self-produced dataset, the authors further analyze the spatial and temporal evolution of land cover and soil erosion, revealing a pronounced overall reduction in erosion intensity over the study period. The long-term and high-frequency observations enable novel insights into the seasonal heterogeneity of erosion driven by precipitation, the role of vegetation dynamics in erosion mitigation, and the influence of topographic factors. In addition, the attempt to assess potential erosion under an optimized vegetation configuration provides practical implications for soil conservation and land management strategies in the region.

The manuscript is clearly written and accompanied by high-quality data visualizations. Overall, this study makes a valuable contribution in terms of both data products and analytical perspectives, and I believe it is suitable for publication after revisions.

Reply: Thank you so much for your positive comments. We believed the manuscript is much improved after addressing your comments. Below, please find our point-to-point response.

Reviewer Comment 1.1 — The land-cover dataset developed in this study is directly applied to soil erosion estimation, while the land-cover products referenced in the Introduction and used for accuracy comparison are mostly general-purpose datasets with coarse thematic categories and broad spatial coverage. Given the strong dependence of soil erosion modeling on land-cover characteristics, it would be helpful to clarify whether any land-cover datasets specifically designed for soil erosion assessment have been developed or applied in the Loess Plateau region. If such erosion-oriented land-cover datasets exist, how do their spatial resolution and mapping accuracy compare with the proposed LP-QLC10 dataset?

Table R1: Quantitative results of the land-cover products on the time-series valuation points.

Datasets	Metrics	2001	2006	2011	2016	2021	Average
CLCDs	OA	0.737	**0.791**	0.759	0.790	0.781	0.7716
GLC_FCS30D		0.753	0.743	0.757	0.749	0.742	0.7488
YRCC_LPLC		0.707	0.752	0.757	0.791	0.784	0.7582
Esri_GLC10		–	–	–	–	0.744	–
LP-QLC10 (ours)		**0.785**	0.787	**0.800**	**0.855**	**0.845**	**0.8144**
CLCDs	Kappa	0.610	0.668	0.651	0.685	0.669	0.6566
GLC_FCS30D		0.648	0.621	0.663	0.645	0.633	0.6420
YRCC_LPLC		0.583	0.625	0.654	0.694	0.682	0.6476
Esri_GLC10		–	–	–	–	0.611	–
LP-QLC10 (ours)		**0.686**	**0.673**	**0.715**	**0.783**	**0.772**	**0.7258**
CLCDs	FWIoU	0.523	0.609	0.566	0.589	0.594	0.5762
GLC_FCS30D		0.556	0.548	0.555	0.556	0.570	0.5570
YRCC_LPLC		0.512	0.570	0.564	0.600	0.604	0.5700
Esri_GLC10		–	–	–	–	**0.739**	–
LP-QLC10 (ours)		**0.663**	**0.643**	**0.582**	**0.647**	0.692	**0.6454**

Table R2: Quantitative results of the land-cover products on the publicly available validation points.

Datasets	SinoLC-1 (7382 points in 2020)			Geo-wiki (1183 points in 2012)		
	OA	Kappa	FWIoU	OA	Kappa	FWIoU
CLCDs	0.696	0.559	0.520	0.480	0.311	0.317
GLC_FCS30D	0.662	0.529	0.501	0.475	0.307	0.326
YRCC_LPLC	0.706	0.581	0.535	0.496	0.330	0.334
Esri_LC10	0.699	0.555	0.623	–	–	–
LP-QLC10 (ours)	**0.798**	**0.709**	**0.660**	**0.505**	**0.346**	**0.357**

Reply: Thank you for this insightful comment. To further demonstrate the advantages of our proposed dataset, we included an additional published dataset specifically developed for land-cover change analysis on the Loess Plateau for both quantitative and qualitative comparisons. In the Loess Plateau region, most existing land-cover datasets are general-purpose products developed at national or global scales[R1,R2] and are not specifically designed for soil erosion assessment. Although several studies[R3,R4] have produced land-use or erosion-related land-cover information at local or catchment scales, these datasets typically have limited spatial coverage or insufficient temporal continuity, which constrains their consistent application in large-scale, long-term analyses such as the entire Loess Plateau.

In addition, YRCC_LPLC[R5] was developed specifically for the Loess Plateau to characterize land-cover changes induced by ecological restoration and provides annual land-cover maps at 30 m resolution from 1990 to 2022. Following the suggestion, we included YRCC_LPLC in our comparative evaluation and updated the quantitative and qualitative results. As shown in Table R1, the multi-year validation indicates that YRCC_LPLC performs comparably to national-scale 30 m products such as CLCDs, achieving an average OA of 0.7582. In contrast, our LP-QLC10 achieves superior quantitative performance, with an average OA of 0.8144. Moreover, the evaluation based on third-party sample points further supports this conclusion,

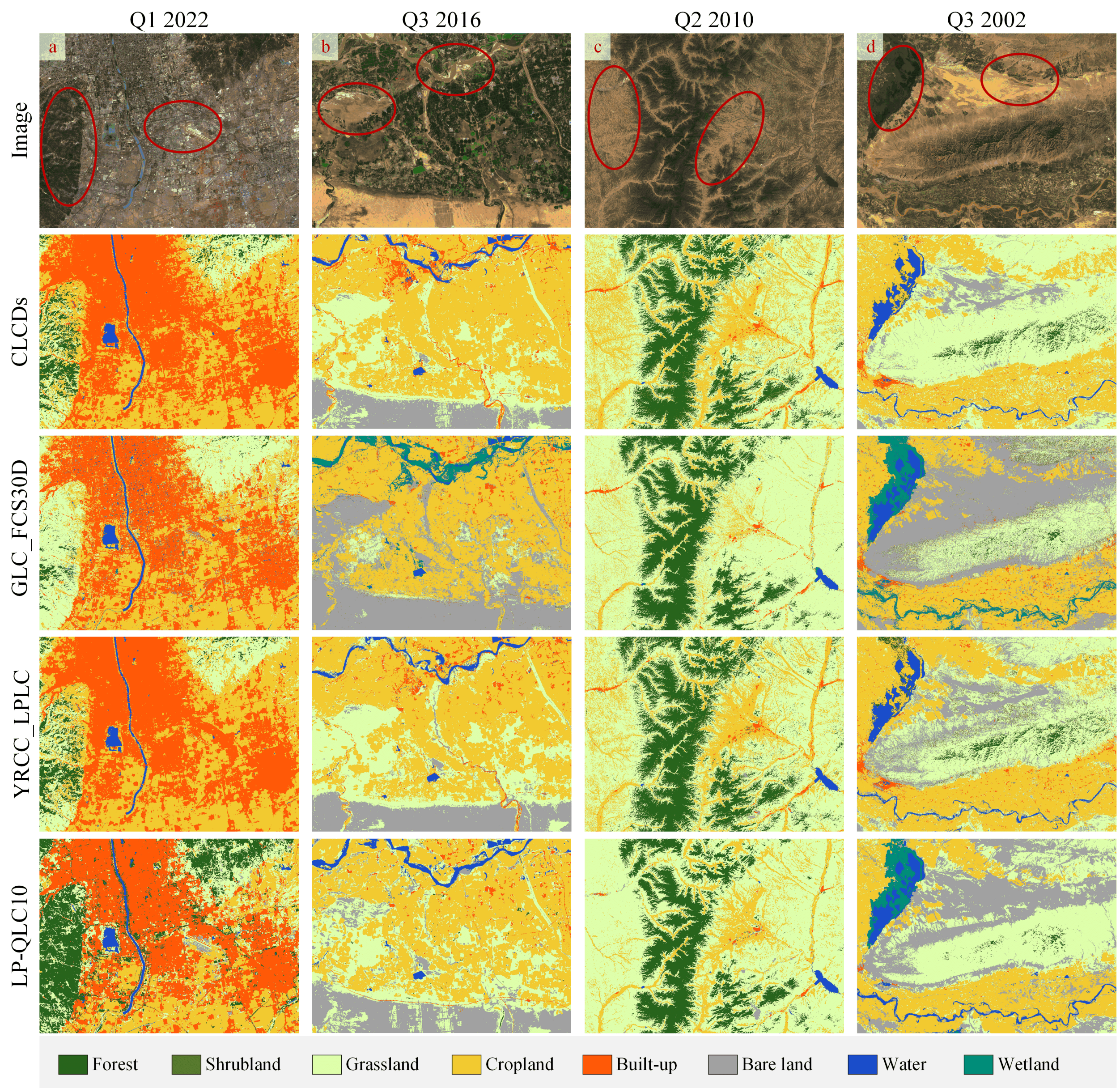

Figure R1: Visual comparison of land-cover classification results over four representative regions: (a) urban areas, (b) agricultural zones, (c) mountainous regions, and (d) wetlands. The satellite images in the figure are from © Google Earth.

as shown in Table R2, where LP-QLC10 outperforms the other datasets across all three metrics. In addition to improving overall classification accuracy, LP-QLC10 is designed with soil-erosion applications in mind, emphasizing the reliable representation of erosion-relevant surface characteristics and their seasonal dynamics. In particular, the quarterly temporal resolution enables the dataset to capture intra-annual variability in vegetation cover types such as cropland and grassland, which directly influences erosion-related processes and associated modeling factors. These design features make LP-QLC10 particularly suitable for long-term, large-scale soil erosion studies in the Loess Plateau, where consistent classification, temporal stability, and the ability to resolve seasonal land-surface dynamics are essential.

Meanwhile, we have also added the visualization results of YRCC_LPLC to the qualitative comparison, as shown in Fig. R1. YRCC_LPLC exhibits patterns similar to those of CLCDs. Specifically, it shows noticeable confusion among forest, grassland, and cropland in transitional landscapes that characterized by fragmented land parcels. In addition, YRCC_LPLC does not include wetlands in its classification system, which limits its ability to represent wetland-related land-surface characteristics.

In the revised manuscript, comparison results have been modified and presented in Tables 3, 4, and Figure 7 in Section 4.1 and 4.2.

Reference of this reply:

[R1] Zhang, X., Zhao, T., Xu, H., Liu, W., Wang, J., Chen, X. and Liu, L., 2024. GLC_FCS30D: the first global 30 m land-cover dynamics monitoring product with a fine classification system for the period from 1985 to 2022 generated using dense-time-series Landsat imagery and the continuous change-detection method. Earth System Science Data, 16(3), pp.1353-1381.

[R2] Yang, J. and Huang, X., 2021. The 30 m annual land cover dataset and its dynamics in China from 1990 to 2019. Earth System Science Data, 13(8), pp.3907-3925.

[R3] Tian, P., Tian, X., Geng, R., Zhao, G., Yang, L., Mu, X., Gao, P., Sun, W. and Liu, Y., 2023. Response of soil erosion to vegetation restoration and terracing on the Loess Plateau. Catena, 227, p.107103.

[R4] Klik, A. and Rosner, J., 2020. Long-term experience with conservation tillage practices in Austria: Impacts on soil erosion processes. Soil and Tillage Research, 203, p.104669.

[R5] Wang, Z., Shi, X., Dou, S., Cheng, M. and Miao, L., 2025. The 30 m land cover dataset for capturing land cover changes induced by ecological restoration from 1990 to 2022 on the Chinese Loess Plateau. Scientific Data, 12(1), p.252.

Reviewer Comment 1.2 — The land-cover mapping in this study is based on eight categories. Please clarify the rationale for selecting these specific categories. In particular, it would be helpful to explain how these categories are relevant to soil erosion research and whether they are designed to effectively represent erosion-related surface characteristics.

Reply: Thank you for this question. The eight land-cover categories were selected based on their functional relevance to soil erosion processes rather than purely thematic or land-use considerations. In soil-erosion research, the key concern is how different surface types regulate rainfall interception, surface runoff generation, soil exposure, and human disturbance. Accordingly, these categories represent major erosion-related surface characteristics across the Loess Plateau, including vegetation-covered surfaces with different protective capacities (e.g., forest, shrubland, and grassland), cultivated land with active human disturbance (e.g., cropland), exposed or weakly protected surfaces (e.g., bare land), and surfaces where water erosion is negligible or not applicable (e.g., water and wetlands). Built-up areas are treated separately due to their distinct hydrological and erosion responses associated with surface hardening. This classification scheme strikes a balance between physical interpretability and temporal consistency over long time series.

Moreover, the selected categories are directly compatible with soil-erosion modeling frameworks such as RUSLE, in which land-cover classes are mapped to erosion-related parameters, particularly the cover management factor (C) and the support practice factor (P). Specifically, according to ecological specification of China[R1], C factor is determined by land-cover category and Fractional Vegetation Cover (FVC), as summarized in Table R3 and Eq. 1, and all land-cover types required by this standard are included in the LP-QLC10 classification system. Meanwhile, the P factor is assigned based on land cover category and slope class, as detailed in Table R4. Therefore, the eight-category classification is not only physically

Table R3: C factor values under different levels of Fractional Vegetation Cover (FVC).

Category	FVC					
	<0.1	0.1–0.3	0.3–0.5	0.5–0.7	0.7–0.9	>0.9
Forest	0.100	0.080	0.060	0.020	0.004	0.001
Shrubland	0.400	0.220	0.140	0.085	0.040	0.011
Grassland	0.450	0.240	0.150	0.090	0.043	0.011
Bare land	0.700					
Built-up	0.010					

Table R4: P factor values assigned to different land-cover types and slopes.

Category	Slope (°)	P
Forest	-	1
Shrubland	-	0.29
Grassland	-	0.41
	0–5	0.49
	5–7	0.59
	7–9	0.65
Cropland	9–12	0.70
	12–20	0.81
	20–24	0.95
	>24	1
Built-up	-	0
Bare land	-	1
Water	-	0
Wetland	-	0

meaningful for erosion mechanisms, but also ensures straightforward for long-term soil erosion modeling on the Loess Plateau.

$$C_{\text{crop}} = 0.221 - 0.595 \log c. \qquad (1)$$

Reference of this reply:

[R1] Ministry of Ecology and Environment of the People's Republic of China (MEE). Technical Specification for Investigation and Assessment of National Ecological Status: Ecosystem Services Assessment. Tech. Rep. HJ 1173–2021, Beijing, China, 2021 (in Chinese).

Reviewer Comment 1.3 — The imagery used for land-cover mapping is derived from multiple satellite sources (e.g., Landsat and Sentinel) and forms dense temporal sequences. To improve the transparency and usability of the dataset, it is recommended to provide a concise visualization of the image acquisition timeline, such as stacked bar charts or timeline histograms showing the temporal distribution of input images. Displaying acquisition dates in this way would help users better understand data availability, temporal coverage, and seasonal sampling characteristics, thereby facilitating more effective use of the dataset.

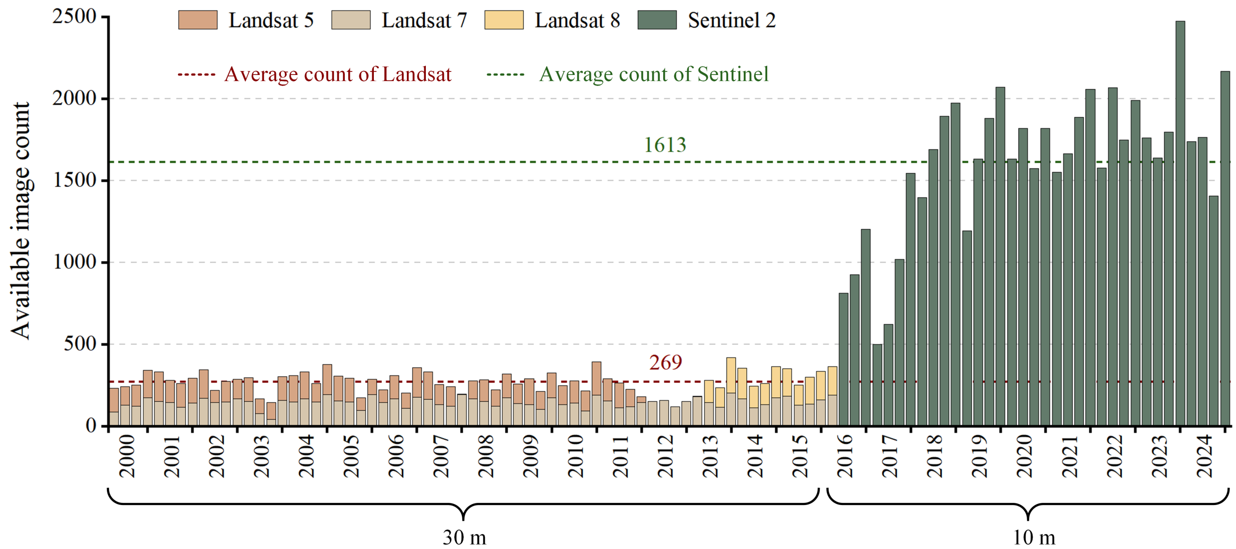

Figure R2: The obtained image count from multiple platforms within each temporal period. The statistic denotes the number of quality-screened satellite image tiles in Google Earth Engine that intersect the Loess Plateau. A Landsat scene covers approximately 3.3×10^4 km^2, whereas a Sentinel tile covers approximately 1.0×10^4 km^2.

Reply: Thank you for your comments. We compiled statistics on the acquired data counts and dates from multiple platforms and illustrated them in figure to clarify the data distribution. Specifically, during the data collection phase, we divided the time span into three consecutive months, corresponding to the four quarters of each year. For each period, we retrieved all available imagery from the Google Earth Engine (GEE) platform and applied a median compositing strategy to generate a single representative image for that quarter. Because median composites rely on the number of valid observations, the quantity of available images directly affects the robustness and quality of the synthesized quarterly image. Therefore, for each period, we reported the number of available images from each satellite as a reference for data availability.

The acquisition period and the number of available images are illustrated in Figure R2. From 2000 to 2016, the quarterly composites were generated using the Landsat series, combining observations from different sensors (e.g., Landsat 5, 7, and 8, depending on the year). After 2016, we used Sentinel-2 imagery. The statistics indicate that, over the Loess Plateau, the Landsat series provides about 300 usable images per quarter, whereas Sentinel-2 provides approximately 1600 tiles per quarter, substantially increasing the sampling density. Consequently, the Sentinel-2 observations not only provide finer spatial resolution (10 m) but also a higher observation frequency, together enabling more robust median compositing and supporting higher-quality, more spatially complete land-cover mapping after 2016.

In the revised manuscript, the statistical details are presented in Section 2.2 and Figure A2 as follows: *“The acquisition periods and the number of images used from multiple platforms are detailed in Figure A2.”*

Reviewer Comment 1.4 — Given the long-term and high-frequency nature of the proposed land-cover and soil erosion dataset, the manuscript would benefit from a more explicit discussion on how these results could be translated into policy-relevant applications. In particular, it is recommended that the authors clarify how the dataset and the identified erosion patterns could support practical decision-making at the policy level, such as evaluating the effectiveness of existing soil conservation measures, and guiding ecological restoration planning in the Loess Plateau.

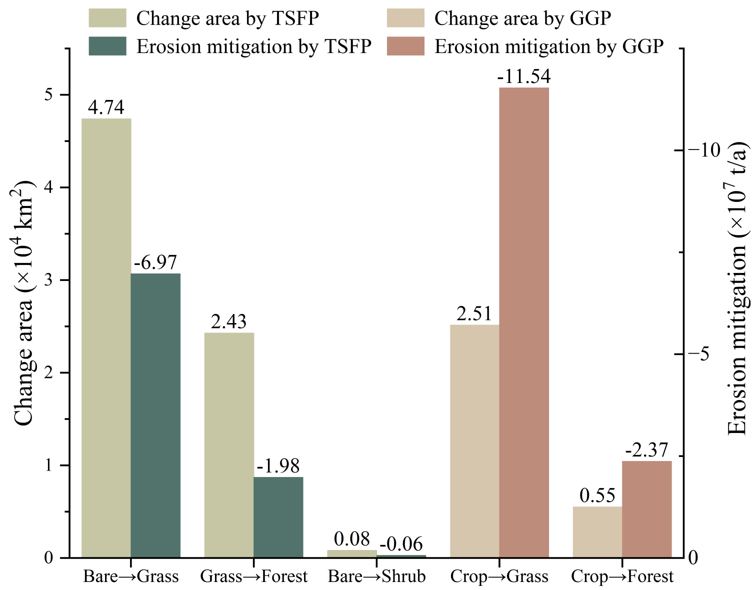

Figure R3: The land-cover changes and associated soil-erosion mitigation from 2000 to 2024, driven by major national programs including the Three-North Shelter Forest Program (TSFP) and the Grain for Green Program (GGP).

Reply: Thanks for the constructive comments. To further analyze the impact of policies on the Loess Plateau region, we explore the progress achieved in policy-guided soil erosion mitigation and identify areas where governance requires further improvement. First, we quantified the land-cover change area and the associated erosion reduction of major vegetation transitions from 2000 to 2024. In this region, ecological restoration has been primarily guided by two national programs: the Three-North Shelter Forest Program (TSFP) [R1] and the Grain for Green Program (GGP) [R2]. Based on the objectives and implementation focus of these policies, we attribute major land-cover transitions to the two programs: transitions from bare land to grassland, grassland to forest, and bare land to shrubland are mainly associated with TSFP, whereas transitions from cropland to grassland and cropland to forest are mainly associated with GGP. We note that these attributions may not capture all land-cover changes across the entire Loess Plateau, as additional environmental drivers and local human activities also contribute to observed transitions. Nevertheless, this rule-based attribution provides a practical way for policy evaluation using the proposed LP-QLC10 dataset, and offers a quantitative reference for assessing restoration effectiveness.

As illustrated in Figure R3, the TSFP primarily promotes the conversion of bare land to grassland (4.74×10^4 km^2) and grassland to forest (2.43×10^4 km^2) across the Loess Plateau, with a smaller extent of bare land converting to shrubland. Among these transitions, the conversion from bare land to grassland yields substantial erosion mitigation, reducing soil loss by -6.97×10^7 t/a. In contrast, although the land-cover changes associated with the GGP occur over a smaller total area, their erosion-mitigation benefits are more pronounced. The cropland-to-grassland transition covers 2.51×10^4 km^2 and reduces erosion by -11.54×10^7 t/a. The area of cropland-to-forest transition is 0.55×10^4 km^2, yet it decreases erosion by -2.37×10^7 t/a. Overall, the estimated erosion reduction attributed to the GGP is about 1.5 times that attributed to the TSFP over 2000–2024.

Second, based on the land-cover pattern in Q4 2024, we generated an optimized land-cover map un-

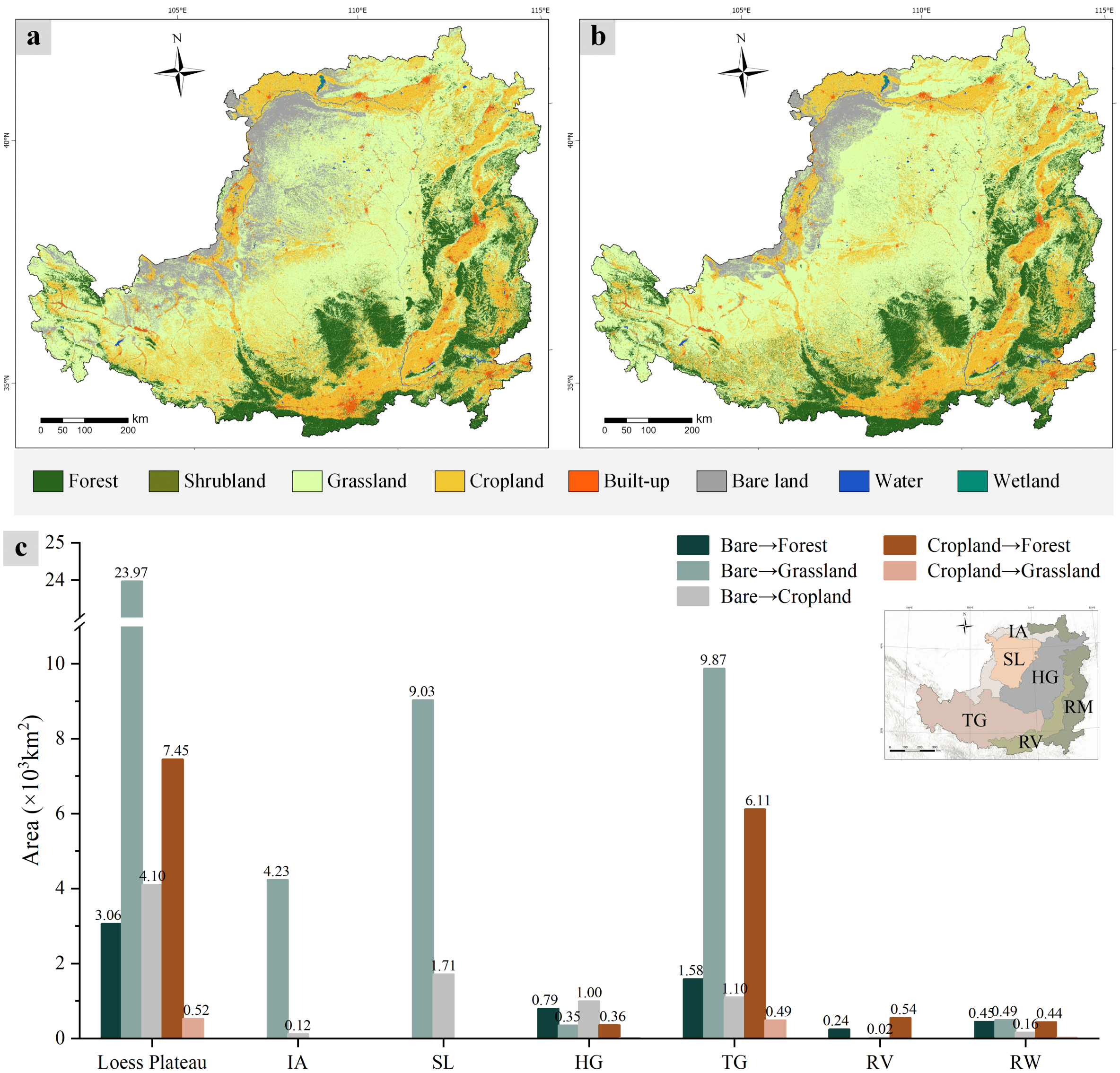

Figure R4: Potential minimum soil erosion in the Loess Plateau. (a) Current soil erosion in 2024, (b) estimated minimum soil erosion under optimized land-cover conditions, and (c) statistical distribution of erosion intensity levels.

der the environmental suitability constraints defined in Section 5.2 of the manuscript. Compared with the current land-cover pattern in Fig. R4(a), the optimized map in Fig. R4(b) indicates substantial landscape adjustments, and a detailed statistical summary of the changes is provided in Fig. R4(c). The transitions from the current state to the minimum-erosion scenario can also be grouped according to the two national programs. Specifically, bare-to-forest and bare-to-grassland transitions are consistent with the primary objectives of the TSFP, whereas cropland-to-forest and cropland-to-grassland transitions align with the GGP. In addition, bare-to-cropland serves as a compensatory change to offset cropland losses in the optimized scenario. Among these transitions, bare-to-grassland under the TSFP accounts for the largest changing area, requiring an additional 2.4×10^4 km^2 conversion. Meanwhile, under the GGP, cropland-to-forest represents a particularly challenging transition: not only it involves an area of 7×10^3 km^2, but the establishment of forest cover typically requires sustained management over years to decades, requiring long-term planning and continuous implementation.

In the revised manuscript, we added a paragraph in Section 5.1 to analyze the effectiveness of existing soil conservation measures: *"As illustrated in Figure 14(b), the TSFP primarily promotes the conversion of bare land to grassland (4.74×10^4 km^2) and grassland to forest (2.43×10^4 km^2) across the Loess Plateau, with a smaller extent of bare land converting to shrubland. Among these transitions, conversion from bare land to grassland yields substantial erosion mitigation (-6.97×10^7 t/a, ranging -7.66– -6.50$\times 10^7$ t/a considering the land-cover uncertainty). In contrast, although the land cover changes associated with the GGP occur over a smaller total area, their erosion mitigation benefits are more pronounced. The cropland to grassland transition covers 2.51×10^4 km^2 and reduces erosion by -11.54×10^7 t/a. The cropland to forest transition covers only 0.55×10^4 km^2, yet it decreases erosion by -2.37×10^7 t/a. Overall, the estimated erosion reduction attributed to the GGP is approximately 1.5 times that attributed to the TSFP over 2000–2024."*

The suggestion for future ecological restoration is modified in Section 5.2 as follows: *"Bare to forest and bare to grassland transitions are consistent with the primary objectives of the TSFP, whereas cropland to forest and cropland to grassland transitions align with the GGP. In addition, bare to cropland serves as a compensatory adjustment to offset cropland losses in the optimized scenario. Among these transitions, bare to grassland under the TSFP accounts for the largest converted area (2.4×10^4 km^2), concentrated in the central Plateau, including the SL and TG regions. Meanwhile, under the GGP, cropland to forest represents a particularly challenging transition: it not only involves 7×10^3 km^2, but also typically requires sustained management over years to decades to establish stable forest cover, underscoring the need for long-term planning and continued implementation."*

Reference of this reply:

[R1] Zhai, J., Wang, L., Liu, Y., Wang, C. and Mao, X., 2023. Assessing the effects of China's three-north shelter forest program over 40 years. Science of the Total Environment, 857, p.159354.

[R2] Lei, D.E.N.G., Shangguan, Z.P. and Rui, L.I., 2012. Effects of the grain-for-green program on soil erosion in China. International Journal of Sediment Research, 27(1), pp.120-127.